Bounds on Phase and Frequency Estimation from 1-bit Quantized Signals with Phase Dithering

Martin Schlüter, Meik Dörpinghaus, and Gerhard P. Fettweis
Vodafone Chair Mobile Communications Systems, SFB 912 HAEC,
Technische Universität Dresden, Dresden, Germany,
{martin.schlueter, meik.doerpinghaus, gerhard.fettweis}@tu-dresden.de

***Abstract*—Designing digital receivers based on 1-bit quantization and oversampling w.r.t. the transmit signal bandwidth enables lower power consumption and a reduced circuit complexity compared to conventional amplitude quantization, since high resolution in time domain is less difficult to achieve than high resolution in amplitude domain. However, standard receiver synchronization algorithms cannot be applied, since 1-bit quantization is a highly non-linear function.**

This paper is a first step to understand the influence of 1-bit quantization on the estimation of the channel parameters (e.g., timing, phase, and frequency offset). We will derive the Fisher Information (FI) matrix of phase and frequency, considering a known timing error and white Gaussian noise. Moreover, we propose to apply a uniformly distributed phase dither at the receiver, prior to 1-bit quantization, in order to reduce the non-linear effect. The same effect can be achieved in practice by sampling at a low intermediate frequency. We obtain analytical results for the FI matrix with uniform phase dithering at the receiver and derive tight closed form upper bounds for the low and high SNR case.

I. Introduction

With the increasing demand for faster communication systems, soon data rates in the terabit per second regime are required. It has recently been understood that analog-to-digital conversion forms a bottleneck at the receiver w.r.t. the power consumption. In particular in wireless short range scenarios, e.g., communication between computer boards [1], [2] an analog-to-digital converter (ADC) with a sampling rate of multiple gigasamples per second has a major impact on the overall power consumption of the wireless link. An annually compiled survey on recent advances in ADC design shows that power limited high sampling rates come at the price of coarse quantization [3]. Having this in mind, using an ADC with 1-bit quantization can be beneficial as the low resolution can be compensated by higher sampling rates. It was reported in [2, Section IV.D-E] that 1-bit quantization and oversampling is still more energy-efficient than conventional high resolution sampling at Nyquist rate, since neither an automatic gain control, nor linear amplification is required.

Numerical studies have found that when using suitable modulation schemes and sequence design, oversampling is beneficial in terms of the achievable rate [4], [5]. Moreover, a bound on the achievable rate of the continuous time (i.e., infinite oversampling) additive white Gaussian noise (AWGN) channel with 1-bit output quantization and strict bandlimitation was derived in [6]. These analytical results confirmed the aforementioned numerical studies. On the other hand, literature on synchronization with 1-bit quantization at the receiver is still very rare. In [7] the joint synchronization of phase and frequency in a QPSK and Nyquist rate based communication system with coarse phase quantization and perfect timing was considered.

However, a full investigation on joint timing, phase, and frequency synchronization has not been conducted yet. In order to understand the problem under 1-bit quantization, a first step is to analyze the fundamental limits of channel parameter estimation, which are determined by the Fisher Information (FI) and the Cramér-Rao lower bound (CRLB). Unfortunately, oversampling w.r.t. signal bandwidth results in noise correlation and it is a mathematically open problem to find an analytical description for the likelihood function of system models with colored Gaussian noise and 1-bit quantization, since there is no analytical description of the orthant probabilities [8]. Thus a lower bound on the FI was derived that requires only the first and second order moments [9], [10].

Unfortunately, this bound can only be computed numerically and is thus not well suited for the purpose of understanding the effect of 1-bit quantization on the channel parameter estimation. Hence, in this work we will consider white noise by adapting the receive filter bandwidth to the sampling frequency. Based on the example of phase estimation, it was shown in [10] that this method is inferior to considering colored noise, since increasing the receive filter bandwidth increases the noise power, and thus decreases the SNR. Hence, for white noise the performance loss compared to the unquantized case converges to the low SNR limit of $\frac{2}{\pi}$ [11], [12] when the oversampling rate is increasing. If the receive filter bandwidth is fixed to the bandwidth of the transmit signal, the noise is correlated and oversampling can decrease the performance loss beyond $\frac{2}{\pi}$ [10]. However, considering white noise allows for an analytical treatment and it is known from the unquantized case that the system with colored noise behaves very similar to the system with white noise [13, Chapter 6.2].

This paper takes an important step into understanding the impact of 1-bit quantization by computing the FI matrix of phase and frequency, considering a known timing error. We will show that the performance of the parameter estimation from complex valued signals is strongly influenced by the phase of the signal. Therefore, we propose a uniform phase dither to remove this dependence and give analytical results

for the average FI. In order to obtain closed form solutions, we derive tight upper bounds on the FI (i.e., lower bounds on the CRLB) for the cases of low and high SNR.

II. System Model

We consider the linearly modulated transmit signal

$$u(t) = \sum_{n=-(N/2)}^{(N/2)-1} a_n g\left(t - nT - \epsilon T\right). \tag{1}$$

The N symbols $\{a_n\}$ are chosen from an arbitrary signal constellation over the complex plane and $g(t)$ is the impulse response of the pulse shaping filter of single sided bandwidth $W_g = \frac{\alpha+1}{2T}$, where T is the symbol duration and $\alpha \in [0,1]$ is the roll-off factor. Our derivations do not require a specific pulse form, but for numerical evaluations we consider raised-cosine pulses. Moreover, the pulse $g(t)$ contains a time shift $\epsilon \in [-0.5, 0.5]$ w.r.t. the time reference of the receiver, which we assume to be known in the present work. This signal is modulated onto the carrier frequency f_c, where it is disturbed by white Gaussian noise with power spectral density $N_0/2$. Furthermore, the channel introduces a deterministic but unknown phase rotation ϕ and frequency offset Ω. At the receiver the signal is demodulated and filtered with a rectangular receive filter of single sided bandwidth $W_r \geq W_g$. The receiver samples with a period of T_s and introduces a known phase dither φ_k such that the sampled receive signal is given by

$$\begin{aligned} r_k &= s_k + \eta_k \\ &= \sum_{n=-(N/2)}^{(N/2)-1} a_n g\left(kT_s - nT - \epsilon T\right) e^{j(\Omega k T_s + \phi + \varphi_k)} + \eta_k, \end{aligned} \tag{2}$$

where η_k is zero mean circularly-symmetric complex Gaussian noise with independent real and imaginary part and covariance matrix

$$\left[\mathbf{R}_\eta\right]_{ij} = 2N_0 W_r \mathrm{sinc}\left(2W_r T_s \left|j-i\right|\right). \tag{3}$$

If we match the receive filter bandwidth to the sampling period, i.e., $W_r = 1/(2T_s)$, the noise is white with $\mathbf{R}_\eta = (N_0/T_s)\mathbf{I} = \sigma^2\mathbf{I}$. In this case, the SNR is given by $\mathrm{SNR} = \frac{E_s}{N_0/T_s} = \frac{E_s}{\sigma^2}$, where $E_s = \mathrm{E}\left[a_n^* a_n\right] \int |g(t)|^2 dt$ is the symbol energy. Since the noise is circularly-symmetric, it is not influenced by the phase dithering. In case of 1-bit quantization, the receiver only has access to

$$y_k = \mathrm{sign}\left(\mathrm{Re}\left\{r_k\right\}\right) + j \cdot \mathrm{sign}\left(\mathrm{Im}\left\{r_k\right\}\right) \tag{4}$$

with the signum function

$$\mathrm{sign}\left(x\right) = \begin{cases} 1 & x > 0 \\ -1 & x \leq 0 \end{cases}. \tag{5}$$

In the subsequent sections, we will denote $\mathbf{r}$ as the vector that contains the $2K = MN$ samples r_k, where $M = \frac{T}{T_s}$ is the oversampling factor w.r.t. the symbol rate. Other sample vectors are named accordingly. Moreover, we consider the following assumptions: $\{a_n\}$ is a random sequence of N statistically independent known symbols, the phase dither realizations φ_k are known, and $\varphi_k = 0$ in the unquantized case.

III. Fisher Information

For the unquantized observation vector $\mathbf{r}$, the FI matrix is given by

$$\left[\mathbf{F}_\mathbf{r}\right]_{\theta_i\theta_j} = 2\mathrm{Re}\left\{\frac{\partial \mathbf{s}^H}{\partial\theta_i}\mathbf{R}_\eta^{-1}\frac{\partial \mathbf{s}}{\partial\theta_j}\right\}, \tag{6}$$

where $\boldsymbol{\theta} = [\phi, \Omega]$ is the vector of the parameters that shall be estimated. For any unbiased estimator $\hat{\boldsymbol{\theta}}(\mathbf{r})$, the variance is lower bounded by the CRLB

$$\mathrm{Var}\left[\hat{\theta}_i(\mathbf{r})\right] \geq \left[\mathbf{F}_\mathbf{r}^{-1}\right]_{\theta_i\theta_i}. \tag{7}$$

In case of white noise, statistically independent known symbols $\{a_n\}$, large N, and a symmetrical summation interval [13, Chapter 6.2], one obtains the fairly simple closed form solutions[1]

$$\left[\mathbf{F}_\mathbf{r}\right]_{\phi\phi} = \frac{2}{\sigma^2}\sum_{k=-K}^{K-1} s_k^* s_k = 2\frac{E_s}{N_0}N, \tag{8}$$

$$\left[\mathbf{F}_\mathbf{r}\right]_{\Omega\Omega} = \frac{2}{\sigma^2}\sum_{k=-K}^{K-1} k^2 T_s^2 s_k^* s_k = 2\frac{E_s}{N_0}\frac{T^2}{12}N^3, \tag{9}$$

and

$$\left[\mathbf{F}_\mathbf{r}\right]_{\phi\Omega} = \frac{2}{\sigma^2}\sum_{k=-K}^{K-1} k T_s s_k^* s_k = 2\frac{E_s}{N_0}N\epsilon T, \tag{10}$$

where (10) only holds for symmetric transmit pulses, i.e., $|g(t)| = |g(-t)|$. Moreover, the cross term $\left[\mathbf{F}_\mathbf{r}\right]_{\phi\Omega}$ is only relevant for very short observation intervals, i.e., $\left[\mathbf{F}_\mathbf{r}^{-1}\right]_{\phi\phi} \approx \left[\mathbf{F}_\mathbf{r}\right]_{\phi\phi}^{-1}$ and $\left[\mathbf{F}_\mathbf{r}^{-1}\right]_{\Omega\Omega} \approx \left[\mathbf{F}_\mathbf{r}\right]_{\Omega\Omega}^{-1}$ for large N.

From [10] we know that the FI matrix of $\mathbf{y}$ (i.e., after quantization) under white Gaussian noise is given by

$$\begin{aligned} \left[\mathbf{F}_\mathbf{y}\right]_{\theta_i\theta_j} &= \frac{1}{\pi\sigma^2} \\ &\times \sum_{k=-K}^{K-1}\left(\frac{e^{-\frac{\left(\mathrm{Re}\left\{s_k\right\}\right)^2}{\sigma^2/2}}\frac{\partial}{\partial\theta_i}\mathrm{Re}\left\{s_k\right\}\frac{\partial}{\partial\theta_j}\mathrm{Re}\left\{s_k\right\}}{Q\left(\frac{\mathrm{Re}\left\{s_k\right\}}{\sigma/\sqrt{2}}\right)Q\left(-\frac{\mathrm{Re}\left\{s_k\right\}}{\sigma/\sqrt{2}}\right)}\right. \\ &\left. + \frac{e^{-\frac{\left(\mathrm{Im}\left\{s_k\right\}\right)^2}{\sigma^2/2}}\frac{\partial}{\partial\theta_i}\mathrm{Im}\left\{s_k\right\}\frac{\partial}{\partial\theta_j}\mathrm{Im}\left\{s_k\right\}}{Q\left(\frac{\mathrm{Im}\left\{s_k\right\}}{\sigma/\sqrt{2}}\right)Q\left(-\frac{\mathrm{Im}\left\{s_k\right\}}{\sigma/\sqrt{2}}\right)}\right), \end{aligned} \tag{11}$$

with $Q(x)$ being the Gaussian Q-function. Since there is no closed form of the likelihood function under correlated Gaussian noise and 1-bit quantization, only a numerically computed lower bound on the FI can be given in this case [9], [10]. Since our aim is to derive simple expressions for the FI in order to understand the impact of 1-bit quantization on the channel parameter estimation performance, we will restrict the discussion in this paper to the case of white noise.

In [7] and [10] the problem of phase estimation in QPSK signaling was studied. It was found that the parameter estimation accuracy is highly dependent on the phase of the receive signal. If the samples r_k are close to the decision boundary in the complex plane, the FI is high, but when the samples lie

[1] As we consider large N, we omitted all terms of order $\mathcal{O}(N)$ in (9).

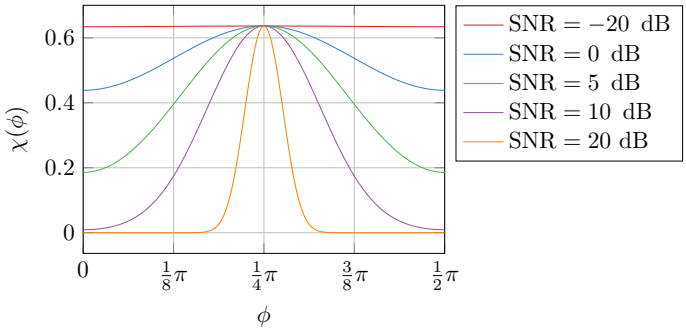

Fig. 1. FI ratio $\chi(\phi)$ of a single QPSK symbol (i.e., $N = 1$) with $T_s = T$, $\varphi_k = 0$ and ϵ and Ω are known to be zero.

within the middle of a quadrant, the FI is low. The higher the SNR, the more pronounced is this effect. This is intuitive, since at high SNR with every sample r_k the same 1-bit quantized measurement y_k would be observed, which results in a poor estimation performance. In Fig. 1 this effect is illustrated by the loss function

$$\chi(\phi) = \frac{[\mathbf{F_y}]_{\phi\phi}}{[\mathbf{F_r}]_{\phi\phi}} \tag{12}$$

for the observation of a single QPSK symbol. We see that the phase dependency is high for high SNR and vanishes for low SNR, where $\chi(\phi) = \frac{2}{\pi}$, a fact well known [11], [12].

In order to remove the phase dependency, we propose the application of uniformly distributed phase dither φ_k such that $\arg(s_k) \sim \mathcal{U}[0, 2\pi]$. Due to the law of large numbers, for large N this dithering will remove the phase dependency of the FI since the phases of the samples s_k are uniformly distributed around the unit circle. As practical implementation of the phase dither we propose low intermediate frequency (IF) sampling, i.e., $\varphi_k = kT_s\Omega_{\text{IF}}$. If Ω_{IF} is chosen such that the receive signal is rotating at least once around the unit circle within the observation interval, low IF sampling has the same effect as a random dither. Moreover, since the receiver knows Ω_{IF}, it also knows φ_k, as we considered in our system model. Thus, the remainder of this paper is concerned with the derivation of closed form expressions for the FI and CRLB of ϕ and Ω under white noise, 1-bit quantization and uniform phase dithering.

IV. Fisher Information with Phase Dithering

In order to enable an analytical treatment in the following derivations, we will give a very close approximation to (11). Since the function $Q(x)Q(-x)$ is very close to a Gaussian function we will use

$$\frac{e^{-x^2}}{Q(x)Q(-x)} \approx c_1 e^{-c_2 x^2}, \tag{13}$$

where c_1 and c_2 are constants that are obtained by numerically solving

$$[c_1, c_2] = \arg\min_{c_1,c_2} \int_0^R \left| \frac{e^{-x^2}}{Q(x)Q(-x)} - c_1 e^{-c_2 x^2} \right| dx. \tag{14}$$

For $R = 10$ we obtain the values $c_1 = 4.0360$ and $c_2 = 0.3930$, which do not change for the considered numerical accuracy if we choose R even higher. The absolute approximation error, shown in Fig. 2, is very small for all values of x, with a maximum of 0.036 at $x = 0$. On the other hand, for large x we observe that the error is larger than the approximated function. However, this does not pose a problem in our case. With (13) we can now approximate (11) with

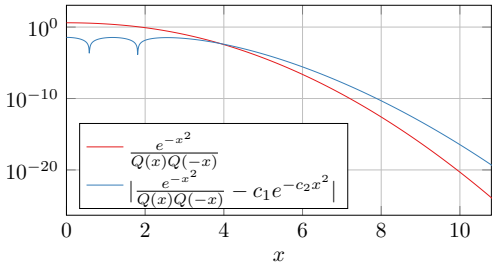

Fig. 2. Absolute approximation error

$$\begin{aligned}\left[\tilde{\mathbf{F}}_{\mathbf{y}}\right]_{\theta_i\theta_j} &= \frac{c_1}{\pi\sigma^2} \\ &\times \sum_{k=-K}^{K-1} \left(e^{-c_2 \frac{(\text{Re}\{s_k\})^2}{\sigma^2/2}} \frac{\partial}{\partial\theta_i}\text{Re}\{s_k\} \frac{\partial}{\partial\theta_j}\text{Re}\{s_k\} \right. \\ &\left. + e^{-c_2 \frac{(\text{Im}\{s_k\})^2}{\sigma^2/2}} \frac{\partial}{\partial\theta_i}\text{Im}\{s_k\} \frac{\partial}{\partial\theta_j}\text{Im}\{s_k\} \right).\end{aligned} \tag{15}$$

In the signal model (2), the estimation parameter vector is defined as $\boldsymbol{\theta} = [\phi, \Omega]$ and with

$$\begin{aligned} s_k &= u_k e^{j(\Omega k T_s + \phi + \varphi_k)} \\ &= \left[\text{Re}\{u_k\}\cos(\Omega k T_s + \phi + \varphi_k) \right. \\ &\quad \left. - \text{Im}\{u_k\}\sin(\Omega k T_s + \phi + \varphi_k)\right] \\ &\quad + j\left[\text{Re}\{u_k\}\sin(\Omega k T_s + \phi + \varphi_k) \right. \\ &\quad \left. + \text{Im}\{u_k\}\cos(\Omega k T_s + \phi + \varphi_k)\right] \end{aligned} \tag{16}$$

we easily obtain

$$\begin{aligned} \frac{\partial}{\partial\phi}\text{Re}\{s_k\} &= -\text{Im}\{s_k\} = -|s_k|\sin(\arg(s_k)) \\ \frac{\partial}{\partial\phi}\text{Im}\{s_k\} &= \text{Re}\{s_k\} = |s_k|\cos(\arg(s_k)). \end{aligned} \tag{17}$$

Likewise, one can easily see that

$$\begin{aligned} \frac{\partial}{\partial\Omega}\text{Re}\{s_k\} &= -kT_s\text{Im}\{s_k\} = -kT_s|s_k|\sin(\arg(s_k)) \\ \frac{\partial}{\partial\Omega}\text{Im}\{s_k\} &= kT_s\text{Re}\{s_k\} = kT_s|s_k|\cos(\arg(s_k)). \end{aligned} \tag{18}$$

From now on we will use the notation $\arg(s_k) = \gamma_k$ such that

$$\begin{aligned}\left[\tilde{\mathbf{F}}_{\mathbf{y}}\right]_{\phi\phi} = \frac{c_1}{\pi\sigma^2} \sum_{k=-K}^{K-1} \left(e^{-c_2 \frac{|s_k|^2\cos^2(\gamma_k)}{\sigma^2/2}} |s_k|^2 \sin^2(\gamma_k) \right. \\ \left. + e^{-c_2 \frac{|s_k|^2\sin^2(\gamma_k)}{\sigma^2/2}} |s_k|^2 \cos^2(\gamma_k) \right).\end{aligned} \tag{19}$$

Our aim is now to obtain an analytical result for the average $\text{E}_{\gamma_k}\left[\left[\tilde{\mathbf{F}}_{\mathbf{y}}\right]_{\phi\phi}\right]$, which is attained by (19) for large N, due to

uniform phase dither and the law of large numbers. To this end, we need to solve the integrals

$$\frac{1}{2\pi}\int_0^{2\pi} e^{-c_2\frac{|s_k|^2\cos^2(\gamma_k)}{\sigma^2/2}}\sin^2(\gamma_k)\,d\gamma_k \tag{20}$$

and

$$\frac{1}{2\pi}\int_0^{2\pi} e^{-c_2\frac{|s_k|^2\sin^2(\gamma_k)}{\sigma^2/2}}\cos^2(\gamma_k)\,d\gamma_k. \tag{21}$$

In order to solve these integrals, we introduce the following Lemma.

Lemma 1: For $x \in \mathbb{C}$

$$\begin{aligned}\int_0^{2\pi} e^{-x\cos^2(\gamma)}\sin^2(\gamma)\,d\gamma &= \pi e^{-\frac{x}{2}}\left(I_0\left(\frac{x}{2}\right)+I_1\left(\frac{x}{2}\right)\right)\\ &= \int_0^{2\pi} e^{-x\sin^2(\gamma)}\cos^2(\gamma)\,d\gamma,\end{aligned} \tag{22}$$

where $I_v(x)$ are the modified Bessel functions of the first kind.

The proof of Lemma 1 is given in the Appendix. The application of approximation (13) above allows us to apply Lemma 1 such that for large N

$$\left[\tilde{\mathbf{F}}_{\mathbf{y}}\right]_{\phi\phi} \approx \mathrm{E}_{\gamma_k}\left[\left[\tilde{\mathbf{F}}_{\mathbf{y}}\right]_{\phi\phi}\right] = \frac{1}{\pi\sigma^2}\sum_{k=-K}^{K-1}\kappa\left(\frac{|s_k|^2}{\sigma^2}\right)|s_k|^2, \tag{23}$$

where

$$\kappa(x) = c_1 e^{-c_2 x}\left(I_0(c_2 x)+I_1(c_2 x)\right). \tag{24}$$

To the best of our knowledge, it would not have been possible to find a closed form solution for $\kappa(x)$ without the approximation (13). Using (17) and (18), and applying the same derivation steps, we obtain for large N

$$\left[\tilde{\mathbf{F}}_{\mathbf{y}}\right]_{\Omega\Omega} \approx \frac{1}{\pi\sigma^2}\sum_{k=-K}^{K-1}\kappa\left(\frac{|s_k|^2}{\sigma^2}\right)k^2T_s^2|s_k|^2 \tag{25}$$

and

$$\left[\tilde{\mathbf{F}}_{\mathbf{y}}\right]_{\phi\Omega} \approx \frac{1}{\pi\sigma^2}\sum_{k=-K}^{K-1}\kappa\left(\frac{|s_k|^2}{\sigma^2}\right)kT_s|s_k|^2. \tag{26}$$

At first we find that (23), (25) and (26) are independent of ϕ and Ω, but are still dependent on the data symbols $\{a_n\}$ through $|s_k|$. However, we are more interested in the average $\mathrm{E}_{\{a_n\}}\left[\left[\tilde{\mathbf{F}}_{\mathbf{y}}\right]_{\theta_i\theta_j}\right]$, which has no closed form solution to the best of our knowledge. Nevertheless, due to the law of large numbers, the FI will attain its average $\mathrm{E}_{\{a_n\}}\left[\left[\tilde{\mathbf{F}}_{\mathbf{y}}\right]_{\theta_i\theta_j}\right]$ for any random sequence $\{a_n\}$, if N is large. Thus, we can estimate the average $\mathrm{E}_{\{a_n\}}\left[\left[\tilde{\mathbf{F}}_{\mathbf{y}}\right]_{\theta_i\theta_j}\right]$ by computing $\left[\tilde{\mathbf{F}}_{\mathbf{y}}\right]_{\theta_i\theta_j}$ for a single long random sequence $\{a_n\}$.

In Fig. 3 we show $\left[\tilde{\mathbf{F}}_{\mathbf{y}}^{-1}\right]_{\phi\phi}$ and $\left[\tilde{\mathbf{F}}_{\mathbf{y}}\right]_{\phi\phi}^{-1}$ exemplary for the parameters $\alpha = 0.5$, $T = 1$, $M = 2$, and $\epsilon = 0.5$. We chose $\epsilon = 0.5$ because we observed that the cross term $\left[\tilde{\mathbf{F}}_{\mathbf{y}}\right]_{\phi\Omega}$ vanishes for symmetric pulses and $\epsilon = 0$, like in the unquantized case (10). Based on $\left[\tilde{\mathbf{F}}_{\mathbf{y}}^{-1}\right]_{\phi\phi}$ we see that only for very small N, the cross term $\left[\tilde{\mathbf{F}}_{\mathbf{y}}\right]_{\phi\Omega}$ is of relevance. The

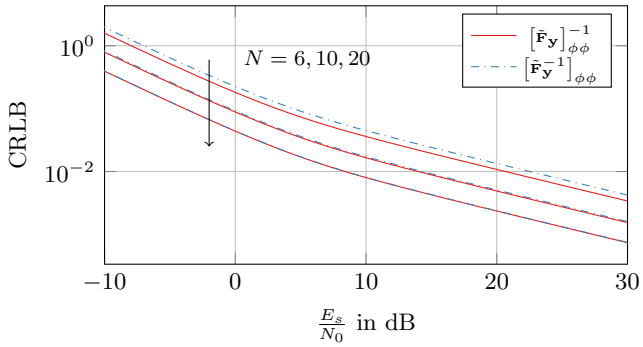

Fig. 3. Comparing $\left[\tilde{\mathbf{F}}_{\mathbf{y}}\right]_{\phi\phi}^{-1}$ and $\left[\tilde{\mathbf{F}}_{\mathbf{y}}^{-1}\right]_{\phi\phi}$ for $\alpha = 0.5$, $T = 1$, $M = 2$, and $\epsilon = 0.5$.

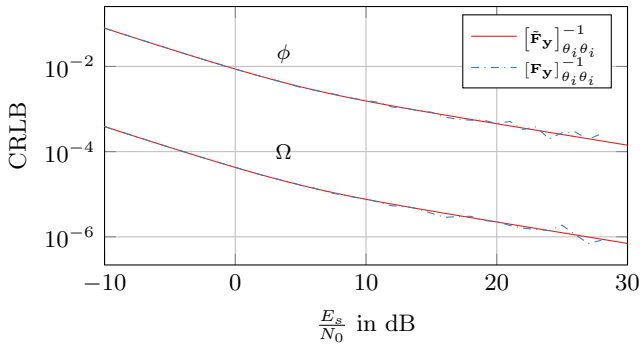

Fig. 4. Comparing $\left[\tilde{\mathbf{F}}_{\mathbf{y}}\right]_{\theta_i\theta_i}^{-1}$ and $[\mathbf{F}_{\mathbf{y}}]_{\theta_i\theta_i}^{-1}$. The system parameters are $N = 100$, $\alpha = 0.5$, $T = 1$, $M = 2$, and $\epsilon = 0.5$.

same observation can be made for $\left[\tilde{\mathbf{F}}_{\mathbf{y}}^{-1}\right]_{\Omega\Omega}$, but we omitted the curves to keep the figure clear. Thus, like in the unquantized case, one can omit $\left[\tilde{\mathbf{F}}_{\mathbf{y}}\right]_{\phi\Omega}$ when computing the CRLB for sufficiently large N. Furthermore, in Fig. 4 we compare $\left[\tilde{\mathbf{F}}_{\mathbf{y}}\right]_{\theta_i\theta_i}^{-1}$ and $[\mathbf{F}_{\mathbf{y}}]_{\theta_i\theta_i}^{-1}$ both obtained from a single random sequence $\{a_n\}$ and uniform phase dither in the latter. We obverse that the obtained analytical results for phase dithering using the approximation (13) are accurate. Furthermore, high SNR requires larger N to average out the phase dependency than low SNR, since the phase dependency increases with increasing SNR. If we increase N, the deviations of the blue dashed curves in the high SNR regime will vanish.

V. Low and High SNR Bounds

Although we found a closed form solution for the average behavior under uniform phase dither, there is no closed form solution to the sums in (23) and (25) that gives the average behavior over all possible sequences $\{a_n\}$. Thus we will give closed form low and high SNR upper bounds, i.e., lower bounds on the CRLB. We omit a discussion on the behavior with very small N, and thus do not consider $[\mathbf{F}_{\mathbf{y}}]_{\phi\Omega}$ in this section. A low SNR upper bound is easily obtained, independently of the signal $\mathbf{s}$ and the target estimation parameter θ, using the fact that $\chi(\theta)$ (see (12)) attains its maximum $\frac{2}{\pi}$ at SNR $= 0$ [11], [12], i.e.,

$$[\mathbf{F}_{\mathbf{y}}]_{\theta_i\theta_j} \leq \frac{2}{\pi}[\mathbf{F}_{\mathbf{r}}]_{\theta_i\theta_j}\ \forall i,j. \tag{27}$$

Thus, in the low SNR regime 1-bit quantization does not influence the channel parameter estimation performance, except for a constant loss factor of $\frac{2}{\pi}$.

To obtain an upper bound for high SNR, we first derive an high SNR approximation for (23) and (25). To this end, for $x \to \infty$ we use [14, Eq. (10.30.4)]

$$I_v(x) \approx \frac{e^x}{\sqrt{2\pi x}} \tag{28}$$

such that

$$\kappa(x) \approx \frac{2c_1}{\sqrt{2\pi c_2 x}}. \tag{29}$$

Thus, with $\sigma^2 = \frac{N_0}{T_s}$ we obtain the high SNR approximation

$$\begin{aligned}\left[\tilde{\tilde{\mathbf{F}}}_{\mathbf{y}}\right]_{\phi\phi} &= \frac{1}{\pi\sigma^2}\sum_{k=-K}^{K-1}\frac{2c_1}{\sqrt{2\pi c_2\frac{|s_k|^2}{\sigma^2}}}|s_k|^2 \\ &= \frac{2c_1\sqrt{T_s}}{\sqrt{2N_0\pi^3 c_2}}\sum_{k=-K}^{K-1}|s_k|.\end{aligned} \tag{30}$$

Since there is still no closed form solution to this sum, we exploit that $|s_k| = \sqrt{s_k^* s_k}$, and $\sqrt{\cdot}$ is a concave function. Thus, with Jensen's inequality we obtain

$$\begin{aligned}\left[\tilde{\tilde{\mathbf{F}}}_{\mathbf{y}}\right]_{\phi\phi} &= \frac{2c_1\sqrt{T_s}}{\sqrt{2N_0\pi^3 c_2}}\sum_{k=-K}^{K-1}\sqrt{s_k^* s_k} \\ &\le \frac{2c_1\sqrt{T_s}}{\sqrt{2N_0\pi^3 c_2}}2K\sqrt{\frac{\sum_{k=-K}^{K-1}s_k^* s_k}{2K}} \\ &= \frac{2c_1\sqrt{T_s}}{\sqrt{2N_0\pi^3 c_2}}\sqrt{MN}\sqrt{\frac{N_0}{2T_s}\left[\mathbf{F}_{\mathbf{r}}\right]_{\phi\phi}} \\ &= \frac{2c_1}{\sqrt{2\pi^3 c_2}}\sqrt{\frac{E_s}{N_0}}N\sqrt{M}.\end{aligned} \tag{31}$$

Like in the unquantized case (8) we observe that $\left[\tilde{\tilde{\mathbf{F}}}_{\mathbf{y}}\right]_{\phi\phi}$ is independent of the transmit pulse $g(t)$ and the timing parameter ϵ as well. On the other hand, while it also grows with $\mathcal{O}(N)$, a major difference is that $\left[\tilde{\tilde{\mathbf{F}}}_{\mathbf{y}}\right]_{\phi\phi}$ only grows with $\mathcal{O}\left(\sqrt{\frac{E_s}{N_0}}\right)$ as opposed to $\mathcal{O}\left(\frac{E_s}{N_0}\right)$ in the unquantized case. Furthermore, it grows with $\mathcal{O}\left(\sqrt{M}\right)$, while oversampling has no influence in the unquantized case, see (8). In Fig. 5 we see that the CRLB has different slopes in the low and high SNR case, as predicted by the closed form low and high SNR bounds. Moreover, we observe that oversampling is moving the high SNR bound of the CRLB downwards, which also moves the crossing point with the low SNR bound to a higher $\frac{E_s}{N_0}$ point. This is due to the fact, that oversampling is decreasing the SNR, since the receive filter must be wider if the noise is required to be white as in the present study. However, the low SNR bound is obviously independent of M, see (27).

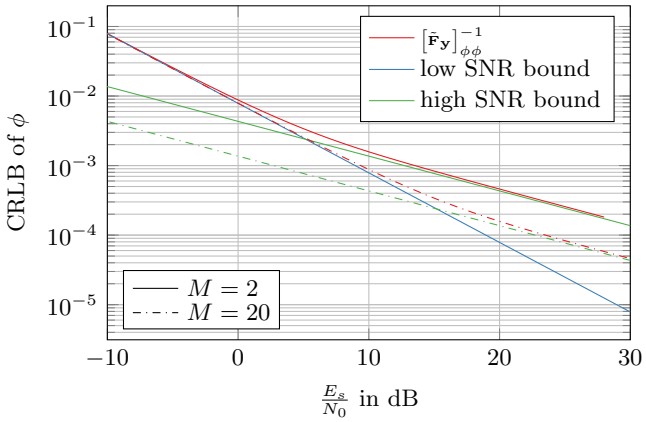

Fig. 5. High and low SNR bounds on $\left[\tilde{\mathbf{F}}_{\mathbf{y}}\right]^{-1}_{\phi\phi}$ for $N = 100$

Using again the high SNR approximation (29) and Jensen's inequality, we obtain

$$\begin{aligned}\left[\tilde{\tilde{\mathbf{F}}}_{\mathbf{y}}\right]_{\Omega\Omega} &= \frac{2c_1\sqrt{T_s}}{\sqrt{2N_0\pi^3 c_2}}\sum_{k=-K}^{K-1}k^2T_s^2\sqrt{s_k^* s_k} \\ &\le \frac{2c_1\sqrt{T_s}}{\sqrt{2N_0\pi^3 c_2}}\left(\sum_{k=-K}^{K-1}k^2T_s^2\right)\sqrt{\frac{\sum_{k=-K}^{K-1}k^2T_s^2 s_k^* s_k}{\sum_{k=-K}^{K-1}k^2T_s^2}} \\ &= \frac{2c_1\sqrt{T_s}}{\sqrt{2N_0\pi^3 c_2}}T_s\sqrt{\sum_{k=-K}^{K-1}k^2}\sqrt{\frac{N_0}{2T_s}\left[\mathbf{F}_{\mathbf{r}}\right]_{\Omega\Omega}}.\end{aligned} \tag{32}$$

Now, using Faulhaber's formula, $K = (MN)/2$, and (9), the RHS of (32) can be bounded by

$$\begin{aligned}\left[\tilde{\tilde{\mathbf{F}}}_{\mathbf{y}}\right]_{\Omega\Omega} &\le \frac{2c_1\sqrt{T_s}}{\sqrt{2N_0\pi^3 c_2}}T_s\sqrt{MN(MN+2)(MN+1)\frac{E_s N^3 T^2}{144T_s}} \\ &= \frac{2c_1}{\sqrt{2\pi^3 c_2}}\sqrt{\frac{E_s}{N_0}}\frac{T_s T}{12}N^2\sqrt{M^3N^2+3M^2N+2M} \\ &= \frac{2c_1}{\sqrt{2\pi^3 c_2}}\sqrt{\frac{E_s}{N_0}}\frac{T^2}{12}N^2\sqrt{MN^2+3N+\frac{2}{M}}.\end{aligned} \tag{33}$$

For large N, it is sufficient to only consider the dominant $\mathcal{O}\left(N^3\right)$ term such that

$$\left[\tilde{\tilde{\mathbf{F}}}_{\mathbf{y}}\right]_{\Omega\Omega} \le \frac{2c_1}{\sqrt{2\pi^3 c_2}}\sqrt{\frac{E_s}{N_0}}\frac{T^2}{12}N^3\sqrt{M}. \tag{34}$$

We observe that like in the case of phase estimation, the major difference to the unquantized case is that $\left[\tilde{\tilde{\mathbf{F}}}_{\mathbf{y}}\right]_{\Omega\Omega}$ only grows with $\mathcal{O}\left(\sqrt{\frac{E_s}{N_0}}\right)$, but in return grows with $\mathcal{O}\left(\sqrt{M}\right)$ while oversampling has no effect in the unquantized case. Fig. 6 shows $\left[\tilde{\mathbf{F}}_{\mathbf{y}}\right]^{-1}_{\Omega\Omega}$ and its bounds. We see that the qualitative behavior is identical to $\left[\tilde{\mathbf{F}}_{\mathbf{y}}\right]^{-1}_{\phi\phi}$, as predicted by the closed form low and high SNR bounds.

VI. Conclusion

The channel parameter estimation performance of a receiver with 1-bit quantization is highly dependent on the phase of

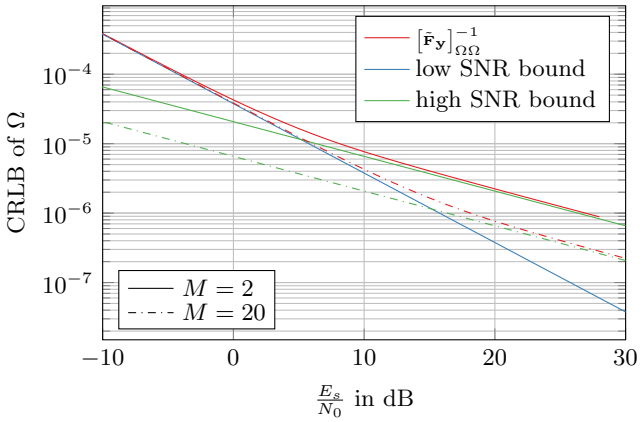

Fig. 6. High and low SNR bounds on $\left[\tilde{\mathbf{F}}_{\mathbf{y}}\right]^{-1}_{\Omega\Omega}$ for $N = 100$ and $T = 1$

the input signal. To overcome this problem, we proposed uniformly distributed phase dithering before 1-bit quantization, which can be implemented in practice by low IF sampling. We analytically derived the FI matrix of phase offset ϕ and frequency offset Ω, considering a known timing error ϵ, white Gaussian noise, and uniform phase dither. Moreover, we derived closed form upper bounds (i.e., lower bounds on the CRLB) for the case of low and high SNR. Compared to the unquantized case, many properties are preserved under uniform phase dithering and 1-bit quantization. The major difference is that for high SNR the FI of ϕ and Ω only grows with $\mathcal{O}\left(\sqrt{\frac{E_s}{N_0}}\right)$ in case of 1-bit quantization, but in return increases with oversampling. This study is a first step to understand the effect of 1-bit quantization on the joint estimation of phase, frequency and timing offset. The presented results will be helpful to understand the more realistic system where also the timing error is unknown and the noise is correlated due to oversampling.

Appendix
Proof of Lemma 1

Proof: With $\cos^2(\gamma) = \frac{1}{2}(1 + \cos(2\gamma))$ and $\sin^2(\gamma) = \frac{1}{2}(1 - \cos(2\gamma))$ we can rewrite the integral on the LHS of (22) to

$$\int_0^{2\pi} e^{-x\cos^2(\gamma)}\sin^2(\gamma)\,d\gamma = \frac{1}{2}e^{-\frac{x}{2}}\left(\int_0^{2\pi} e^{-\frac{x}{2}\cos(2\gamma)}d\gamma - \int_0^{2\pi} e^{-\frac{x}{2}\cos(2\gamma)}\cos(2\gamma)\,d\gamma\right). \tag{35}$$

Now, the first integral on the RHS of (35) solves to

$$\int_0^{2\pi} e^{-\frac{x}{2}\cos(2\gamma)}d\gamma = \frac{1}{2}\int_0^{4\pi} e^{-\frac{x}{2}\cos(t)}dt = 2\pi I_0\left(-\frac{x}{2}\right) = 2\pi I_0\left(\frac{x}{2}\right), \tag{36}$$

where the first equality is obtained with the substitution $t = 2\gamma$, and the second and the third can be found in [14, Chapter 10]. Equivalently, we find that the second integral on the RHS of (35) solves to

$$\int_0^{2\pi} e^{-\frac{x}{2}\cos(2\gamma)}\cos(2\gamma)\,d\gamma = \frac{1}{2}\int_0^{4\pi} e^{-\frac{x}{2}\cos(t)}\cos(t)\,dt = 2\pi I_1\left(-\frac{x}{2}\right) = -2\pi I_1\left(\frac{x}{2}\right), \tag{37}$$

where again the first equality is obtained with the substitution $t = 2\gamma$, and the second and the third can be found in [14, Chapter 10]. If we now put (36) and (37) into (35), we have proved the first equality in (22). The integral in the second equality in (22) can be solved by using exactly the same steps. ■

Acknowledgment

This work is supported by the German Research Foundation (DFG) in the Collaborative Research Center "Highly Adaptive Energy-Efficient Computing", SFB912, HAEC.

References

[1] G. Fettweis, N. ul Hassan, L. Landau, and E. Fischer, "Wireless interconnect for board and chip level," in *Proc. IEEE Des. Autom. Test Eur. Conf. Exhib.*, Grenoble, France, May 2013, pp. 958–963.

[2] G. Fettweis, M. Dörpinghaus, J. Castrillon, A. Kumar, C. Baier, K. Bock, F. Ellinger, A. Fery, F. H. P. Fitzek, H. Härtig, K. Jamshidi, T. Kissinger, W. Lehner, M. Mertig, W. E. Nagel, G. T. Nguyen, D. Plettemeier, M. Schröter, and T. Strufe, "Architecture and advanced electronics pathways toward highly adaptive energy-efficient computing," *Proc. IEEE*, vol. 107, no. 1, pp. 204–231, Jan. 2019.

[3] B. Murmann, "ADC performance survey 1997-2018." [Online]. Available: http://web.stanford.edu/ murmann/adcsurvey.html

[4] L. Landau, M. Dörpinghaus, and G. P. Fettweis, "1-bit quantization and oversampling at the receiver: Sequence-based communication," *EURASIP J. Wirel. Commun. Netw.*, vol. 2018, no. 1, p. 83, Dec. 2018.

[5] L. Landau, M. Dörpinghaus, and G. Fettweis, "1-bit quantization and oversampling at the receiver: Communication over bandlimited channels with noise," *IEEE Commun. Lett.*, vol. 21, no. 5, pp. 1007–1010, May 2017.

[6] S. Bender, M. Dörpinghaus, and G. Fettweis, "On the achievable rate of bandlimited continuous-time 1-bit quantized AWGN channels," in *Proc. IEEE Int. Symp. Inf. Theory*, Aachen, Germany, Jun. 2017, pp. 2083–2087.

[7] A. Wadhwa and U. Madhow, "Near-coherent QPSK performance with coarse phase quantization: A feedback-based architecture for joint phase/frequency synchronization and demodulation," *IEEE Trans. Signal Process.*, vol. 64, no. 17, pp. 4432–4443, Sep. 2016.

[8] A. Genz and F. Bretz, *Computation of Multivariate Normal and t Probabilities*, 1st ed. Berlin Heidelberg: Springer, 2009.

[9] M. Stein, A. Mezghani, and J. A. Nossek, "A lower bound for the Fisher information measure," *IEEE Signal Process. Lett.*, vol. 21, no. 7, pp. 796–799, Jul. 2014.

[10] M. Schlüter, M. Dörpinghaus, and G. P. Fettweis, "Bounds on channel parameter estimation with 1-bit quantization and oversampling," in *Proc. IEEE Int. Work. Signal Process. Adv. Wirel. Commun.*, Kalamata, Greece, Jun. 2018.

[11] M. Stein, A. Kurzl, A. Mezghani, and J. A. Nossek, "Asymptotic parameter tracking performance with measurement data of 1-bit resolution," *IEEE Trans. Signal Process.*, vol. 63, no. 22, pp. 6086–6095, Nov. 2015.

[12] G. Zeitler, G. Kramer, and A. C. Singer, "Bayesian parameter estimation using single-bit dithered quantization," *IEEE Trans. Signal Process.*, vol. 60, no. 6, pp. 2713–2726, Jun. 2012.

[13] H. Meyr, M. Moeneclaey, and S. Fechtel, *Digital Communication Receivers: Synchronization, Channel Estimation, and Signal Processing*. New York, NY, USA: John Wiley & Sons, Inc., 1997.

[14] F. W. Olver, D. W. Lozier, R. F. Boisvert, and C. W. Clark, *NIST Handbook of Mathematical Functions*, 1st ed. New York, NY, USA: Cambridge University Press, 2010.